Polymer Bulletin (2024) 81:7467–7479
https://doi.org/10.1007/s00289-023-05052-5

ORIGINAL PAPER

Physical properties of copper oxide nano-composite incorporated PVP/chitosan blend matrix by casting method

E. M. Abdelrazek[1] · Asmaa M. Elzayat[1] · A. A. Elbana[2] · W. M. Awad[1]

Received: 9 March 2023 / Revised: 23 October 2023 / Accepted: 29 October 2023 /
Published online: 27 November 2023

Abstract

Nanocomposite blend films were prepared by a simple casting method. Polyvinyl propylene (PVP) and chitosan (PVP/chitosan) were used as a based material. Different CuO nanoparticles concentrations were added to a specific blend film concentration of PVP/chitosan (80/20). The mechanism of the interaction between the blend and the nanoparticles was studied by different characterization techniques. The structure modification was confirmed by X-ray diffraction pattern due to the addition of the nanoparticles, in addition, the complexation and the miscibility between the nanoparticles and the blended composite was confirmed by UV–Vis spectroscopy and Fourier transform infrared spectroscopy is by the appearance of new peaks in the spectrum. The band gap computation and optical characteristics show that the addition of the nanoparticles decreases the crystallinity of the nanocomposites system. The findings show that the surface morphology checked by scanning electron microscopy shape and swelling rate behavior are affected by the integration of CuO nanoparticles into the polymer blend matrix. From all the results, this work has a great interest in wide bioapplications such as wound healing and food packing.

Keywords PVP · Chitosan · Copper oxide NPs · Casting method · Swelling rate

✉ Asmaa M. Elzayat
asmaaelzayat25@yahoo.com

✉ W. M. Awad
w.mhmd@yahoo.com

[1] Physics Department, Faculty of Science, Mansoura University, Mansoura 35516, Egypt

[2] Department of Basic Sciences, Higher Institute of Engineering and Technology at Manzala, Mansoura, Egypt

Introduction

The uses of nanocomposite materials that combine inorganic and organic components have attracted more attention nowadays. The incorporation of inorganic materials within the polymeric matrix can enhance its properties [1–3]. Recently, there is a wide range of biopolymers have been used as a platform for that purpose within its matrix for wide applications such as the food industry as active packaging material [2]. Natural polymers are good candidates due to their biodegradability and biocompatibility.

Chitin is deacetylated to produce chitosan, a naturally occurring polyaminosaccharide, which after cellulose is the second-most prevalent polysaccharide [3, 4]. On its chains, it has a lot of NH_2 and OH groups that can act as coordination and reaction sites. Considering that it is a polymer that dissolves in water, polyvinylpyrrolidone (PVP) is nontoxic with excellent transparency, biocompatibility, and film-forming ability and it has been utilized in a broad range of areas, such as medical, food, cosmetics, and health-related domains [5–7]. The best method for creating novel multifunctional materials is through the use of mixed polymers.

The miscibility of chitosan and PVP in the films has been reported and it is considered that carbonyl groups in the pyrrolidone rings of PVP interacts with amino and hydroxyl groups in chitosan by forming hydrogen bonds and producing materials with novel characteristics [8–11]. The rheological behavior of the polymer or its composites under different conditions of preparation control the quality of the material and improving the yield product [12, 13].

Combining inorganic particles with blended polymers is a smart move to improve the material's performance and enable the creation of cutting-edge composite systems that improve the parent polymer's performance. CuONPs, an example of an ionic metal oxide nanoparticle (NPs), are highly intriguing antimicrobial agents because they have a lot of corners and edges, a lot of surface area, and a lot of reactive sites [6, 14–16]. It has a wide range of potential physical properties and combines readily with polymers to give composites unique physicochemical features. With a specific dose, these nanoparticles with their large surface areas and crystalline shapes can have antibacterial effects [17–20]. These composite matrix can be used as well for the removal of the pollutants of water based on the adsorption process and the swelling behavior of the composite manner [21–23]. Copper oxide is commonly used as a nanofiller material in the construction of polymer nanocomposites due to its specific properties, such as its favorable electrical characteristics, low energy gap of 1.85 eV, and ease of manufacturing [24–28].

Composite materials composed of PVP, chitosan, and copper oxide nanoparticles are being actively explored for diverse applications including antimicrobial coatings, wound dressings, tissue engineering scaffolds, drug delivery, and biosensors. The complementary properties of the components can lead to enhanced performance compared to the individual materials. For instance, PVP can improve the dispersion of copper oxide nanoparticles in the chitosan matrix and enhance film flexibility. Chitosan provides antimicrobial effects and biocompatibility to

the nanocomposites. However, there is still limited understanding on how the interactions between PVP, chitosan, and copper oxide nanoparticles affect the stability, morphology, mechanical strength, biocompatibility, and toxicity of the composites [29–32].

In this investigation, the structural, optical, and morphological properties of a PVP/chitosan blend implanted with various CuONPs ratios were examined. A simple casting method, which is a rapid and inexpensive solution to produce a nanocomposite matrix for the prepared samples. The prepared samples' swelling behavior was examined, and the results suggested using the product in industrial settings such food packing.

Experimental section

Materials

Chitosan with a low molecular weight (Sigma-Aldrich, Mv = 50,000–190,000 Da, 75–85% deacetylated) (deacetylation degree: C75%), and polyvinylpyrrolidone PVP (Sigma-Aldrich, ≥ 99%), copper oxide nanoparticle prepared in liquid solution. The received chemicals and solvents were all utilized as directed. Throughout each experiment, ultrapure water was used.

Synthesis of PVP/chitosan nanocomposites blend films

Chitosan and polyvinylpyrrolidone blend matrix were synthesized by a simple casting process. In order to make chitosan solution, 0.2 g of chitosan powder was dissolved in 100 ml of deionized water and 2% acetic acid, followed by 3 h at 45 °C of continuous stirring to create a homogeneous viscous solution. In the same manner, to make the PVP solution, 0.8 g of PVP were dissolved in 100 ml of deionized water. The two separated solutions were mixed and then they continued stirring for 2 h at 40 °C until complete homogeneity was observed. Copper oxide nanoparticles with different ratios have been added to the PVP/chitosan blend mixture. The nanocomposite blends were sonicated using a dip sonicator then they were stirred till the homogeneous distribution of CuONPs into the blend matrix was observed. Finally, The resulting PVP/chitosan mixes, which contained various ratios of CuO nanoparticles, were then placed into plastic Petri plates and dried for a further 36 h at 40 °C in an oven. The schematic representation of the process is described in Fig. 1. The blend films of nanocomposites were discovered to be 0.22 mm thick.

Nanocomposite blend films characterization

Surface morphology and composition. Scanning electron microscopy (SEM) Field Emission Gun microscope, attached with EDX unit (Energy-dispersive x-ray analysis), operating voltage at 20 kV, and magnification 14 × to 1000,000 × were used to examine the surface morphology of the samples. To minimize sample charging

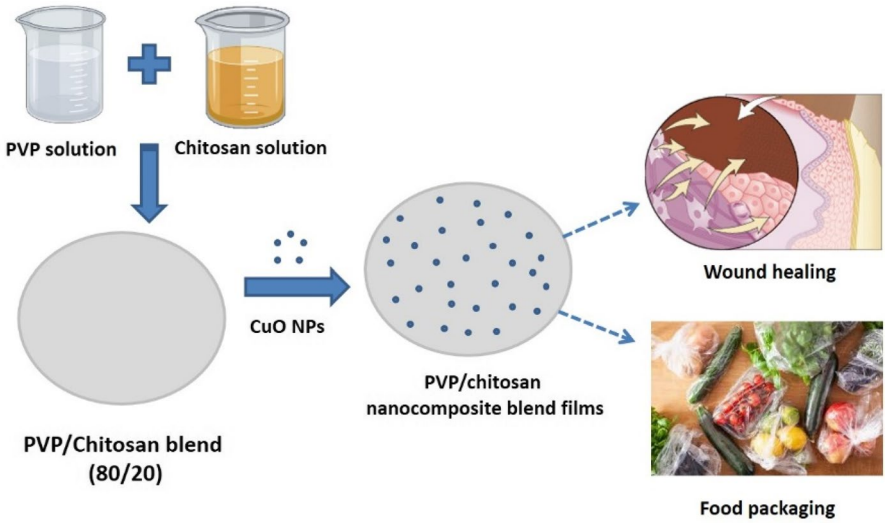

Fig. 1 Schematic representation for the preparation of PVP/chitosan blend nanocomposite films containing CuO NPs by casting method

effects brought on by the electron beam, a thin layer of gold plating was applied to the sample's external surface.

X-ray diffraction scans on a Cu K target with a secondary monochromator wave were performed using a PANalytical XPert PRO XRD system (When the tube operated where $\lambda = 1.540$ at 45 kV–40 mA) (Holland). The Bragg angles are in the range of (5–80). The various crystalline structures in pure and doped films are determined using the peak locations in X-ray diffraction spectra.

Fourier transform infrared spectroscopy (FTIR) was used to analyze the specimens' vibrational mode absorption spectra were acquired for multiple films using a single beam (Nicolet iS10, USA) spectrophotometer with a resolution of 2 cm^{-1} and a spectral range of (4000–400) cm^{-1}.

UV/Vis spectroscopy was measured in the wavelength range of 200–800 nm with a spectrophotometer (V-750, UV–Vis, JASCO, and Japan) to analyze the microstructure of the specimens and their optical properties. It comprises photon spectroscopy in the UV–visible region, which uses visible light as well as contiguous near-UV and near-infrared regions.

Swelling behavior

The swelling behavior was studied by taking pieces from the dried blend compositions with (2 cm x 2 cm) and soaking them in different phosphate buffer solutions

(PBS) at pH (4, 5, 6, 7, 8, and 9) for 24 h at 37 °C till the samples reached equilibrium state of swelling. The swollen films are removed from the insertion media by using filter paper to remove excess liquid from the surface of the samples and weighed. The swelling behavior was studied by Eq. 1 every 2 h for measuring the water uptake of the sample by using an analytical balance.

$$\text{Swelling ratio}\% = \frac{Ws - Wd}{Wd} \times 100 \quad (1)$$

where W_d: is the weight of the dried polymer at 60 °C and W_s: is the weight of the swollen samples in various PBS solutions at 37 °C.

Results and discussion

PVP/chitosan blend nanocomposite blend films by casting method

Nanocomposite blend films of PVP/chitosan matrix doped with copper oxide nanoparticles with different ratios were performed by a simple casting method to develop nanocomposite systems for different applications. This method is simple, performed under mild conditions, and can give a reproducible yield. Copper oxide nanoparticles with different ratios have been added with the PVP/chitosan blend mixture (80/20) as explained in Table 1. The nanocomposite blends were sonicated and they continuous stirring till homogeneous distribution was attained. Finally, The resulting PVP/chitosan mixes, which contained various ratios of CuO nanoparticles, were then placed into plastic Petri plates and dried for a further 36 h at 40 °C in an oven. Table 1 provides a summary of the various blend matrix compositions created in this work.

By using X-ray diffraction, the interaction and complexation between chitosan and PVP were investigated. Figure 2 confirms the miscibility between the blend through the broadening peaks which are characteristics of both polymers. However, in the case of the blends of PVP/Chitosan doped with CuO nanoparticles, the intensity of the peaks decreased gradually with the nanoparticle's concentration till disappeared at higher concentrations and only the diffraction peaks of CuONPs still appeared [24].

Table 1 Samples with different content of CuONPs

Sample	CuONPs wt%
PVP/chitosan (80/20)	0
Cu1	2.5
Cu2	5
Cu3	7.5
Cu4	10
Cu5	12.5

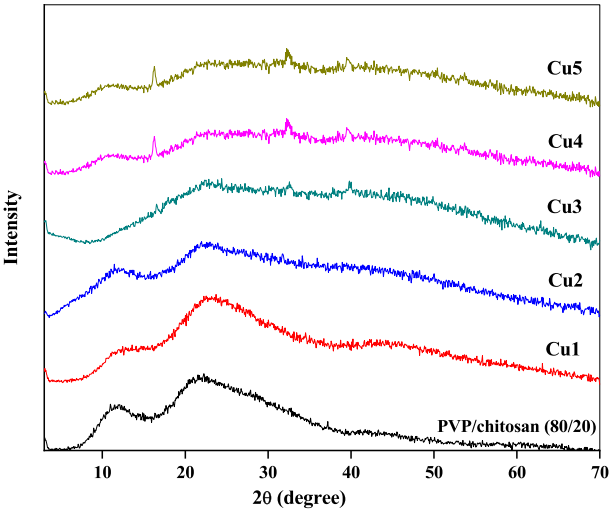

Fig. 2 X-ray diffraction patterns of PVP/chitosan blend and PVP/chitosan nanocomposite films

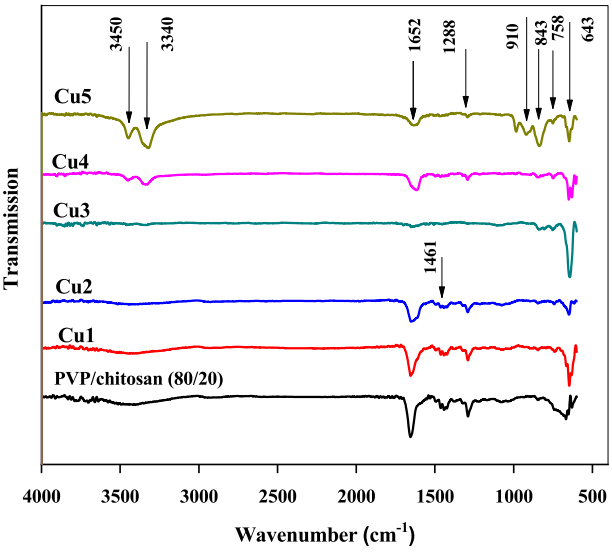

Fig. 3 FTIR spectra of PVP/chitosan polymer blend and PVP/chitosan polymer blend loaded with CuONPs, (The band's shift is indicated by the position and direction of the arrowheads.)

The absorption interaction of the PVP/Chitosan polymer blend and the blend samples containing different concentrations of CuONPs fillers were confirmed by the FTIR spectrum as shown in Fig. 3. The spectrum shows a hydroxyl group (–OH stretching) at 3340 cm^{-1}. Chitosan's spectra at 1652 cm^{-1} showed absorption bands that were attributed to (–C = O) secondary amide stretching. Another band, positioned at the C–H saccharide structure's wagging vibration, is seen at 910 cm^{-1} [33,

34]. The results reveal that the position of the characteristic bands corresponding to single polymers changed and shifted with the addition of the different concentrations of CuO nanoparticles, this was explained by how the dopant and polymeric mix matrix interacted. As the –OH and –NH atoms stretched, the band at 3456 cm^{-1} shifted to 3335 cm^{-1}. Furthermore, the strength and wavenumber of the strong absorption band at 1666 cm^{-1} and the band at 1558 cm^{-1} changed as a result of the hydrogen bonding between the carbonyl group of PVP and the NH_2 group of chitosan [35]. On the other hand, a change in the intensity of the distinctive peaks in the fingerprint region as well as a small alteration in the region 650–550 cm^{-1} were found following the addition of CuO nanoparticles, and it is related to the low concentration of CuO additives.

Optical characterization

Clarifying the electronic band structures and optical constants of crystalline and non-crystalline materials requires research into their optical properties. The absorbance of chitosan, PVP, PVP/chitosan blend, and the blend loaded with CuONPs, scaled in the wavelength 200–900 nm as shown in Fig. 4. On the one hand, the PVP/chitosan composites showed a maximum absorption peak at 225 nm that matched theπ-π^* transition of unsaturated bonds in the polymer mixture [36]. On the other hand, PVP/chitosan blend films containing different contents of CuONPs have a small shift toward higher wavelength. This change could be explained by intermolecular hydrogen interactions between the copper ions and nearby hydrogen groups in the polymer chain, or by hydrogen bonds between the C=O of the mix and the copper ions [34, 37]. A second peak that confirmed the complexation between the polymer blend and the CuONPs filler was also present.

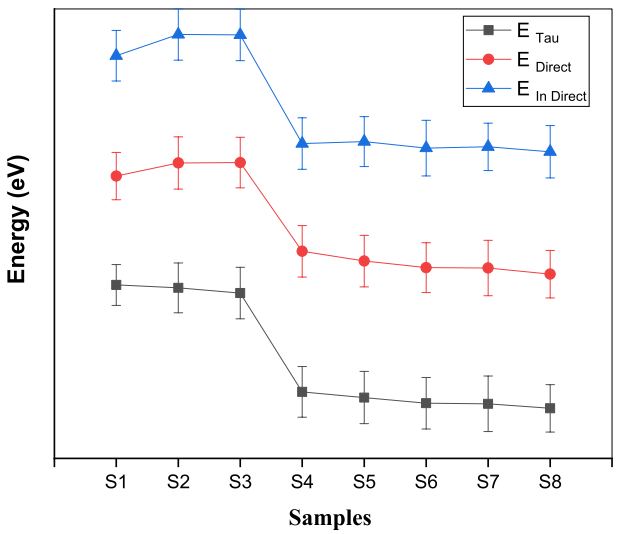

Fig. 4 $E_{Indirect}$, E_{Direct}, and E_{Tauc} for tested samples

The optical band gap (E_g) in the high absorption area can be estimated using the well-known relationship:

$$\alpha h\nu = A\left(h\nu - E_g\right)^n \quad (2)$$

Where $\boldsymbol{\alpha}$ a constant, the exponent n is: has values of 1/2, 2, 3/2, and 3, in accordance with the permitted direct, permitted indirect, prohibited direct, and prohibited indirect excitations and incident photon energy is $h\nu$ [38–41]. Here, only the curve associated with permitted indirect and direct excitation ($n=2$ and 1/2) is shown. The Eg values that are derived from Eq. 2 and shown in Table 2 are a result of the dependence of $(\alpha h\nu)^2$ on $h\nu$, where the extrapolated intercept on the $h\nu$ axis for $(\alpha h\nu)^2$ and $(\alpha h\nu)^{1/2}$ & $h\nu$ plot yields the values.. The optical gap (E_g) of chitosan film is about 4.35 eV which was increased to 5.13 eV for the polymer blend (PVP/chitosan: 80/20). However, the addition of CuONPs with different ratios decreased the values to reach about 2.4 eV and 2 eV for indirect and direct transition. The electrical interactions between the CuO NPs and the host polar mix may be to blame for this decrease in E_g values [37, 38]. In Fig. 4, the amorphous region in the PVP/chitosan blend increases with the addition of CuONPs which in turn affect the disordering [42–45].

Surface morphology (SEM)

The morphology of the different formulations of the nanocomposite thin films of both polymer and polymer/CuONPs prepared via the casting method was studied employing scanning electron microscopy (SEM). The corresponding electron micrographs for the nanocomposite thin films are presented in Fig. 5. It can be observed that PVP/chitosan blend (control sample F1) is homogeneous with a smooth surface. However, the PVP/chitosan containing CuONPs (samples F2, F3, and F4) show a homogeneous distribution of the nanoparticles on the blend surface by generating well-formed spherical particles with a certain roughness on the surface, the result of the presence of copper oxide nanostructures embedded within the blend matrix that is increased by raising the added values of the nanoparticles.

Table 2 Calculated values for E_g, $E_{Direct,}$ and $E_{Indirect}$ for tested samples

Samples	E_g (eV)	E_{Direct}	$E_{Indirect}$
Chitosan	5.3	4.8	4.35
PVP	5.04	4.87	4.87
PVP/chitosan	5.04	5.13	4.86
Cu1	2.6	2.96	2.2
Cu2	2.5	2.72	2.25
Cu3	2.4	2.56	2.09
Cu4	2.36	2.55	2.12
Cu5	2.28	2.4	2

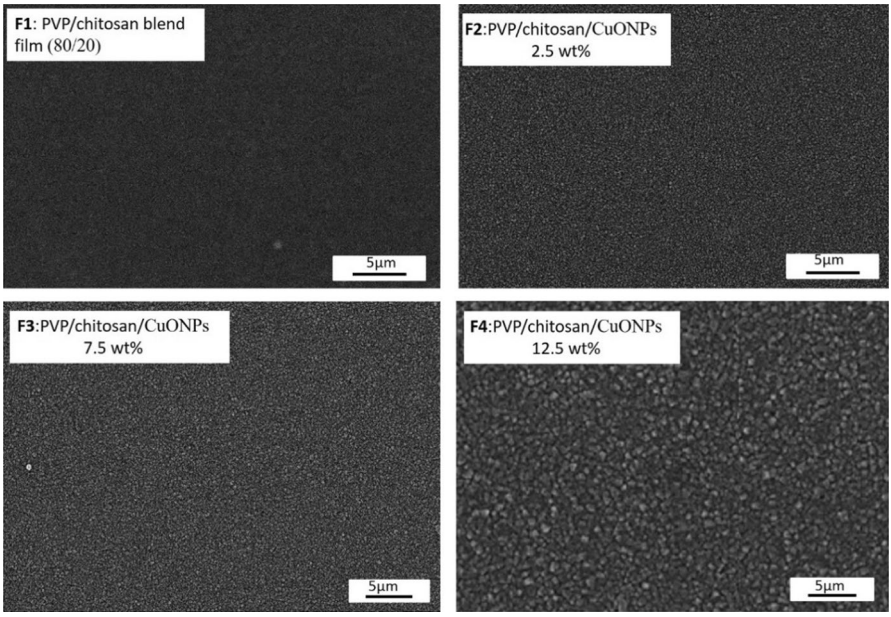

Fig. 5 SEM photographs for PVP/chitosan, and PVP/chitosan/CuONPs with different content

Swelling ratio (SR)

The swelling of the resulting nanocomposite blend films was investigated in various buffered phosphate media (pH = 4, 5, 6, 7, 8, and 9). The associated data are shown in Fig. 6 as a percentage of swelling degree with the pH. The values of the swelling behavior of the samples calculated from Eq. (1). Every sample showed greater

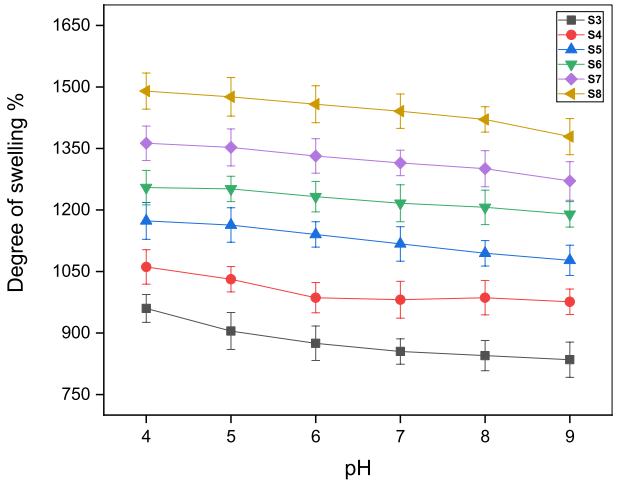

Fig. 6 Swelling degree of PVP/chitosan containing different ratios of CuONPs at different pH

Table 3 Calculated swelling degree at different pH

Samples	Swelling degree%					
	pH4	pH5	pH6	pH7	pH8	pH9
PVP/chitosan	960	875	810	763	745	719
Cu1	905	845	800	760	735	705
Cu2	875	800	777	741	714	687
Cu3	855	795	754	725	697	670
Cu4	845	800	731	715	683	650
Cu5	835	790	714	698	653	608

swelling at an acidic pH and less swelling at a basic pH. This behavior is mainly governed by the dissolution nature of the chitosan matrix at lower pH which in turn affects the swelling behavior of the blend and hence increases the value of the swelling in comparison with the neutral case or at higher pH. Chitosan's protonation of its amino groups ($–NH_2$) to ammonium ions ($–NH_3^+$) is what caused the swelling in acidic environments. Because there were more ionic groups (ammonium ions) and charge repulsion at lower pH, additionally, osmotic pressure dropped while swelling increased. As the pH increases toward basic media, the swelling behavior changes from what it was in the acidic media, and this change is explained by the dense network and compact structure that is brought on by more covalent and physical crosslinks, which eventually results in fewer swelling. The results indicate that by increasing the contents of CuONPs within the blend matrix, the swelling behavior decreased dramatically, which in turn reflex the strong interaction between the CuONPs and the PVP/chitosan blend matrix. which depends on the pH of the medium that is based on the protonation/deprotonation of the interactions between the polymeric layer and nanoparticles distribution within the polymer matrix Table 3.

Conclusion

The PVP/chitosan nanocomposite films with various CuONPs content were prepared via casting method. The process favored the homogeneous distribution of CuONPs with some roughness on the blend surface, attributed to the higher number of nanoparticles. The results indicated that surface area and the swelling behavior of the compositions containing copper oxide nanoparticles depending on the protonation/deprotonation of interaction between the polymeric layer and nanoparticle based on the pH of the media. The bio-nanocomposite film PVP/chitosan containing copper nanoparticles recommended for a multifunctional biomedical and food packaging applications.

Funding Open access funding provided by The Science, Technology & Innovation Funding Authority (STDF) in cooperation with The Egyptian Knowledge Bank (EKB).

Declarations

Conflict of interest The authors declared there is no conflicted of interest.

Ethical approval The authors declared that the manuscript is original not published or considered for publications in any other journal.

References

1. Khalid MY, Arif ZU, Noroozi R, Zolfagharian A, Bodaghi M (2022) 4D printing of shape memory polymer composites: a review on fabrication techniques, applications, and future perspectives. J Manuf Process 81:759–797
2. Elzayat A, Tolba E, Pérez-Pla FF, Oraby A, Muñoz-Espí R (2021) Increased stability of polysaccharide/silica hybrid sub-millicarriers for retarded release of hydrophilic substances. Macromol Chem Phys 9:202100027
3. Aranaz I, Alcántara AR, Civera MC, Arias C, Elorza B, Heras Caballero A, Acosta N (2021) Chitosan: an overview of its properties and applications. Polymers 13(19):3256
4. Li J, Zivanovic S, Davidson PM, Kit K (2010) Characterization and comparison of chitosan/PVP and chitosan/PEO blend films. Carbohyd Polym 79:786–791
5. Kumar R, Mishra I, Kumar G (2021) Synthesis and evaluation of mechanical property of chitosan/PVP blend through nanoindentation-a nanoscale study. J Polym Environ 29:3770–3778
6. van den Broek LAM, Knoop RJI, Kappen FHJ, Boeriu CG (2015) Chitosan films and blends for packaging material. Carbohyd Polym 116:237–242
7. Archana D, Singh BK, Dutta J, Dutta PK (2015) Chitosan-PVP-nano silver oxide wound dressing: in vitro and in vivo evaluation. Int J Biol Macromol 73:49–57
8. Marsano E, Vicini S, Skopińska J, Wisniewski M, Sionkowska A (2004) Chitosan and poly(vinyl pyrrolidone): compatibility and miscibility of blends. Macromol Symp 218:251–260
9. Taheri P, Jahanmardi R, Koosha M, Abdi S (2020) Physical, mechanical and wound healing properties of chitosan/gelatin blend films containing tannic acid and/or bacterial nanocellulose. Int J Biol Macromol 154:421–432
10. Lewandowska K (2011) Miscibility and interactions in chitosan acetate/poly(N-vinylpyrrolidone) blends. Thermochim Acta 517:90–97
11. Poonguzhalia R, Khaleel Bashab S, Sugantha Kumari V (2017) Synthesis and characterization of chitosan-PVP-nanocellulose composites for in-vitro wound dressing application. Int J Biolo Macromol 105:111–120
12. Hsissou R, Dagdag O, Berradi M, El Bouchti M, Assouag M, El Bachiri A, Elharfi A (2019) Investigation of structure and rheological behavior of a new epoxy polymer pentaglycidyl ether pentabisphenol a of phosphorus and of its composite with natural phosphate. SN Appl Sci 1:1–9
13. El-Aouni N, Hsissou R, El Azzaoui J, El Bouchti M, Elharfi A (2020) Synthesis rheological and thermal studies of epoxy polymer and its composite. Chem Data Collect 30:100584
14. Zhang J, Chen K, Ding C, Sun S, Zheng Y, Ding Q, Hong Bo, Liu W (2022) Fabrication of chitosan/PVP/dihydroquercetin nanocomposite film for in vitro and in vivo evaluation of wound healing. Int J Biol Macromol 206:591–604

15. Chin S (1998) A water soluble polymer. Chemical industry Press, China
16. Sangeetha V, Sudha PN (2021) Synthesis and characterization of nano chitosan/PVP/SF for environmental engineering applications. Int J Ambient Energy 42:150–155
17. Cao S, Shi Y, Chen G (1998) Blend of chitosan acetate salt with poly (N-vinyl-2-pyrrolidone): Interaction between chain-chain. Polymer Bulletin 41:553–559
18. Fang L, Goh SH (2000) Miscible chitosan/tertiary amide polymer blends. J Appl Polym Sci 76(12):1785–1790
19. Sionkowska A, Wisniewski M, Skopinska J, Vicini S, Marsano E (2005) The influence of UV irradiation on the mechanical properties of chitosan/poly (vinyl pyrrolidone) blends. Polym Degrad Stab 88(2):261–267
20. Sakurai K, Maegawa T, Takahashi T (2000) Glass transition temperature of chitosan and miscibility of chitosan/poly (N-vinyl pyrrolidone) blends. Polymer 41(19):7051–7056
21. Lebkiri I, Abbou B, Hsissou R, Safi Z, Sadiku M, Berisha A, Lebkiri A (2023) Investigation of the anionic polyacrylamide as a potential adsorbent of crystal violet dye from aqueous solution: equilibrium, kinetic, thermodynamic, DFT, MC and MD approaches. J Mol Liq 372:121220
22. Wang D, Lin Z, Wang T, Yao Z, Qin M, Zheng S, Lu W (2016) Where does the toxicity of metal oxide nanoparticles come from: the nanoparticles, the ions, or a combination of both? J Hazard Mater 308:328–334
23. Kadiri L, Ouass A, Hsissou R, Safi Z, Wazzan N, Essaadaoui Y, Lebkiri A (2021) Adsorption properties of coriander seeds: spectroscopic kinetic thermodynamic and computational approaches. J Mol Liq 343:116971
24. Wu J, Wu Y, Yuan Y, Xia C, Saravanan M, Shanmugam S, Pugazhendhi A (2022) Eco-friendly, green synthesized copper oxide nanoparticle (CuNPs) from an important medicinal plant Turnera subulata Sm. and its biological evaluation. Food Chem Toxicol 168:113366
25. Tamgadge Y et al (2015) Studies on nonlocal optical nonlinearity of Sr–CuO–polyvinyl alcohol nanocomposite thin films. Thin Solid Films 595:48–55
26. Sivasubramanian R, Biji P (2016) Preparation of copper (I) oxide nanohexagon decorated reduced graphene oxide nanocomposite and its application in electrochemical sensing of dopamine. Mater Sci Eng B 210:10–18
27. de Souza VS, da Frota HO, Sanches EA (2018) Polyaniline-CuO hybrid nanocomposite with enhanced electrical conductivity. J Mol Struct 1153:20–27
28. Khaorapapong N, Khumchoo N, Ogawa M (2015) Preparation of copper oxide in smectites. Appl Clay Sci 104:238–244
29. Zhu C, Kwok RT, Lam JW, Tang BZ (2018) Aggregation-induced emission: a trailblazing journey to the field of biomedicine. ACS Appl Bio Mater 1(6):1768–1786
30. Kallepu S, Kavitha M, Yeeravalli R, Manupati K, Jadav SS, Das A, Chandrasekhar S (2018) Total synthesis of desmethyl jahanyne and its lipo-tetrapeptide conjugates derived from parent skeleton as bcl-2-mediated apoptosis-inducing agents. ACS Omega 3(1):63–75
31. Cai Y, Guo J, Chen C, Yao C, Chung SM, Yao J, Kong X (2017) Silk fibroin membrane used for guided bone tissue regeneration. Mater Sci Eng C 70:148–154
32. Ahmed S, Ali A, Sheikh J (2018) A review on chitosan centred scaffolds and their applications in tissue engineering. Int J Biol Macromol 116:849–862
33. Menazea AA, Mahmoud KH, Abdel-Rahim FM (2021) Tailoring modifications in the structural, optical, and electrical conductivity properties of polyvinyl pyrrolidone/chitosan doped with vanadium pentoxide nanoparticles using laser ablation technique. Appl Phys A 127(11):1–9
34. Al Mogbel MS, Elabbasy MT, Mohamed RS, Ghoniem AE, Abd El-Kader MFH, Menazea AA (2021) Improvement in antibacterial activity of Poly Vinyl Pyrrolidone/Chitosan incorporated by graphene oxide NPs via laser ablation. J Polym Res 28(12):1–8
35. Waly AL, Abdelghany AM, Tarabiah AE (2022) A comparison of silver nanoparticles made by green chemistry and femtosecond laser ablation and injected into a PVP/PVA/chitosan polymer blend. J Mater Sci Mater Electron 33(29):23174–23186
36. Jeevanantham V, Hemalatha K, Satheeskumar S (2018) Photodegradation activity of pure, PVP capped and chitosan capped ZnO nanoparticles against azo red dye under UV irradiation. J Ovonic Res 14(4):269–275
37. Elabbasy MT, Abd El-Kader MFH, Ismail AM, Menazea AA (2021) Regulating the function of bismuth (III) oxide nanoparticles scattered in Chitosan/Poly (Vinyl Pyrrolidone) by laser ablation on electrical conductivity characterization and antimicrobial activity. J Market Res 10:1348–1354

38. Makuła P, Pacia M, Macyk W (2018) How to correctly determine the band gap energy of modified semiconductor photocatalysts based on UV–Vis spectra. j phys chem lett 9(23):6814–6817
39. Heiba ZK, Mohamed MB, Ahmed SI, Alhazime AA (2021) Tailoring the optical properties of PVA/PVP blend by doping with Cu/MnS nanoparticles. J Vinyl Add Tech 27(2):410–418
40. Tawansi A, Abdel-Kader HI, El-Zalabany M, Abdel-Razek EM (1994) FeCl 3-doped polyvinylidene fluoride: part i interpolaron hopping and optical properties. J mater sci 29:3451–3457
41. Kumar R, Mishra I, Kumar G (2021) Synthesis and evaluation of mechanical property of chitosan/PVP blend through nanoindentation-a nanoscale study. J Polym Environ 29(11):3770–3778
42. Tuğcu-Demiröz F, Saar S, Kara AA, Yıldız A, Tunçel E, Acartürk F (2021) Development and characterization of chitosan nanoparticles loaded nanofiber hybrid system for vaginal controlled release of benzydamine. Eur J Pharm Sci 161:105801
43. Le Dang Q, Dinh QH, Hong TPT, Thuy DCT, Thi NT, Thu HLT (2021) In-vitro antifungal activities of silver-copper complex/chitosan (Ag-Cu@ CS) nanoparticles synthesized by in-situ encapsulation. Vietnam J Catal Adsorpt 10(1S):24–30
44. Lemma E, Kiflie Z, Kassahun SK (2022) Adsorption of Cr (VI) ion from aqueous solution on acrylamide–grafted starch (Coccinia abyssinicca)–PVA/PVP/chitosan/graphene oxide blended hydrogel: isotherms, kinetics, and thermodynamics studies. Sep Sci Technol 58(2):1–16
45. Owonubi SJ, Agwuncha SC, Malima NM, Sadiku ER, Revaprasadu N (2021) Development of bacterial resistant acrylamide-polyvinylpyrrolidone-metal oxide hydrogel nanocomposites. Mater Today Proc 38:982–987